arXiv:1502.02399v1 [cond-mat.mtrl-sci] 9 Feb 2015

Condensed Matter Physics, 2014, Vol. 17, No 4, 43703: 1–10
DOI: 10.5488/CMP.17.43703
http://www.icmp.lviv.ua/journal

Electrocaloric effect in KH_2PO_4 family crystals

A.S. Vdovych[1], A.P. Moina[1], R.R. Levitskii[1], I.R. Zachek[2]

[1] Institute for Condensed Matter Physics of the National Academy of Sciences of Ukraine, 1 Svientsitskii St., 79011 Lviv, Ukraine
[2] National University “Lviv Polytechnic”, 12 Bandera St., 79013 Lviv, Ukraine

Received May 31, 2014, in final form October 7, 2014

The proton ordering model for the KH_2PO_4 type ferroelectrics is modified by taking into account the dependence of the effective dipole moments on the proton ordering parameter. Within the four-particle cluster approximation we calculate the crystal polarization and explore the electrocaloric effect. Smearing of the ferroelectric phase transition by a longitudinal electric field is described. A good agreement with experiment is obtained.

Key words: *electrocaloric effect, KDP, cluster approximation, polarization*

PACS: *77.84.Fa, 77.70.+a*

1. Introduction

The electrocaloric (EC) effect is the change of temperature of a dielectric at an adiabatic change of the applied electric field. Research in this field is driven by a quest for materials that can be used for efficient, environment-friendly, and compact (on-chip) solid-state cooling devices.

The current state of the art on the electrocaloric effect research for ferroelectrics is well summarized in [1, 2]. At the moment, the largest effect is observed in perovskite ferroelectrics. Thus, in [3] in the $PbZr_{0.95}Ti_{0.05}O_3$ thin film with a thickness of 350 nm in a strong electric field (480 kV/cm) the obtained electrocaloric temperature change is $\Delta T = 12$ K. Ab initio molecular dynamics calculations [4] predict $\Delta T \approx 20$ K in $LiNbO_3$. In the hydrogen bonded ferroelectrics of the KH_2PO_4 (KDP) type, the electrocaloric effect was studied for relatively low fields only. Thus, it has been obtained that $\Delta T \approx 0.04$ K at $E \approx 4$ kV/cm [5], $\Delta T \approx 1$ K at $E \approx 12$ kV/cm [6], and $\Delta T \approx 0.25$ K at T_c and $E \approx 1.2$ kV/cm [7].

Theoretical calculations of the electrocaloric effect in KDP have been made in [8] within the Slater model [9] and in the paraelectric phase only. It is also known that the Slater model gives incorrect results in the ferroelectric phase, and more complicated versions of the proton ordering model are required for an adequate description of these crystals. Thus, the effect of electric field on the physical characteristics of the KDP type crystals, such as polarization, dielectric permittivity, piezoelectric coefficients, elastic constants, has been described within the proton ordering model with the piezoelectric coupling to the shear strain ε_6 [10–12] and with proton tunneling [13] taken into account. However, these theories required, in particular, invoking two different values of the effective dipole moments for the paraelectric and ferroelectric phase [10, 12]. This made impossible a correct description of the system behavior in the fields high enough to smear out the first order phase transition. There is an inner logical contradiction in the model: while no physical characteristic of a crystal should exhibit any discontinuity in the fields above the critical one, there is no smooth transition between the values of model parameters, rigidly set to be different for the two phases.

In the present paper we suggest a way to remove this contradiction. Assuming that the difference between the dipole moments is caused by non-zero values of the order parameter, we modify the proton ordering model accordingly. The field dependences of polarization, smearing of the first order phase transition, and the electrocaloric effect are described.

© A.S. Vdovych, A.P. Moina, R.R. Levitskii, I.R. Zachek, 2014

2. Thermodynamic characteristics

We consider the KDP type ferroelectrics in the presence of an external electric field E_3 applied along the crystallographic axis **c**, inducing the strain ε_6 and polarization P_3. The total model Hamiltonian reads

$$\hat{H} = N\hat{H}_0 + \hat{H}_{\mathrm{s}}\,, \tag{1}$$

where N is the total number of primitive cells. The "seed" energy H_0 corresponds to the sublattice of heavy ions and does not explicitly depend on the proton subsystem configuration. It is expressed in terms of the strain ε_6 and electric field E_3 and includes the elastic, piezoelectric, and dielectric contributions [11]

$$\hat{H}_0 = v\left(\frac{1}{2}c_{66}^{E0}\varepsilon_6^2 - e_{36}^0 E_3\varepsilon_6 - \frac{1}{2}\chi_{33}^{\varepsilon 0}E_3^2\right), \tag{2}$$

where v is the primitive cell volume; c_{44}^{E0}, e_{36}^0, $\chi_{33}^{\varepsilon 0}$ are the "seed" elastic constant, piezoelectric coefficient, and dielectric susceptibility, respectively.

The pseudospin part of the Hamiltonian reads

$$\hat{H}_{\mathrm{s}} = \frac{1}{2}\sum_{qf,q'f'} J_{ff'}(qq')\frac{\sigma_{qf}}{2}\frac{\sigma_{q'f'}}{2} + \hat{H}_{\mathrm{sh}} + \sum_{qf}2\psi_6\varepsilon_6\frac{\sigma_{qf}}{2} - \sum_{qf}\mu_f E_3\frac{\sigma_{qf}}{2} + \hat{H}_E\,. \tag{3}$$

Here, the first term describes the effective long-range interactions between protons, including also indirect lattice-mediated interactions [14, 15]; σ_{qf} is the operator of the z-component of a pseudospin, corresponding to the proton on the f-th hydrogen bond ($f = 1, 2, 3, 4$) in the q-th cell. Its eigenvalues $\sigma_{qf} = \pm 1$ are assigned to two equilibrium positions of a proton on this bond.

In (3), $\hat{H}_{\mathrm{sh}}$ is the Hamiltonian of short-range interactions between protons, which includes terms linear over the strain [11]

$$\begin{aligned}
\hat{H}_{\mathrm{sh}} \;=\; & \sum_q\bigg\{\left(\frac{\delta_s}{8}\varepsilon_6 + \frac{\delta_1}{4}\varepsilon_6\right)(\sigma_{q1} + \sigma_{q2} + \sigma_{q3} + \sigma_{q4}) \\
& + \left(\frac{\delta_s}{8}\varepsilon_6 - \frac{\delta_1}{4}\varepsilon_6\right)(\sigma_{q1}\sigma_{q2}\sigma_{q3} + \sigma_{q1}\sigma_{q2}\sigma_{q4} + \sigma_{q1}\sigma_{q3}\sigma_{q4} + \sigma_{q2}\sigma_{q3}\sigma_{q4}) \\
& + \frac{1}{4}(V + \delta_a\varepsilon_6)(\sigma_{q1}\sigma_{q2} + \sigma_{q3}\sigma_{q4}) + \frac{1}{4}(V - \delta_a\varepsilon_6)(\sigma_{q2}\sigma_{q3} + \sigma_{q4}\sigma_{q1}) \\
& + \frac{U}{4}(\sigma_{q1}\sigma_{q3} + \sigma_{q2}\sigma_{q4}) + \frac{\Phi}{16}\sigma_{q1}\sigma_{q2}\sigma_{q3}\sigma_{q4}\bigg\}.
\end{aligned} \tag{4}$$

Here,

$$V = -\frac{1}{2}w_1\,, \qquad U = \frac{1}{2}w_1 - \varepsilon\,, \qquad \Phi = 4\varepsilon - 8w + 2w_1\,,$$

and ε, w, w_1 are the energies of proton configurations.

The third term in (3) is a linear over the shear strain ε_6 field due to the piezoelectric coupling; ψ_6 is the deformational potential. The fourth term effectively describes the system interaction with the external electric field E_3. Here, μ_f is the effective dipole moment of the f-the hydrogen bond, and

$$\mu_1 = \mu_2 = \mu_3 = \mu_4 = \mu.$$

The fifth term in (3) is introduced in the present paper for the first time. It takes into account the assumed dependence of the effective dipole moment on the order parameter (pseudospin mean value)

$$\hat{H}_E = -\Big(\frac{1}{N}\sum_{q'f'}\frac{\sigma_{q'f'}}{2}\Big)^2\mu' E_3\sum_{qf}\frac{\sigma_{qf}}{2}\,. \tag{5}$$

It is equivalent to a term proportional to $P_3^3E_3$ in a phenomenological thermodynamic potential. Note that the terms like $P_3^2E_3$ are not allowed because of the symmetry considerations, and we keep the Hamiltonian to be linear in the field E_3.

In view of the crystal structure of the KDP type ferroelectrics, the four-particle cluster approximation is most suitable for short-range interactions [15, 16]. Long-range interactions and the term $\hat{H}_E$ are taken into account in the mean field approximation. Thus,

$$\hat{H}_E \approx -12N\mu' E_3\eta^2 \sum_{f=1}^{4} \frac{\sigma_{qf}}{2} + 16N\mu' E_3\eta^3. \tag{6}$$

Combining the fourth term in (3) and the first term in (6), we obtain the following term in the Hamiltonian $-(\mu+12\mu'\eta^2)E_3\sum_{qf}\sigma_{qf}/2$. Effectively, the term $12\mu'\eta^2$ in $(\mu+12\mu'\eta^2)$ describes the jump of the dipole moment at the first order phase transition, its different values for the paraelectric and ferroelectric phase, and its smooth behavior in the fields above the critical one, when there is no jump of η. We can now use a single value of μ for both phases and remove the logical contradiction of the earlier theories, described in Introduction.

Proceeding with the standard calculations of the cluster approximation [10, 12, 16], we obtain the following expression for the proton ordering parameter

$$\eta = \langle\sigma_{q1}\rangle = \langle\sigma_{q2}\rangle = \langle\sigma_{q3}\rangle = \langle\sigma_{q4}\rangle = \frac{m}{D},$$

where

$$\begin{aligned}
&m = \sinh(2z+\beta\delta_s\varepsilon_6) + 2b\sinh(z-\beta\delta_1\varepsilon_6),\\
&D = \cosh(2z+\beta\delta_s\varepsilon_6) + 4b\cosh(z-\beta\delta_1\varepsilon_6) + 2a\cosh\beta\delta_a\varepsilon_6 + d,\\
&z = \frac{1}{2}\ln\frac{1+\eta}{1-\eta} + \beta\nu_c\eta - \beta\psi_6\varepsilon_6 + \frac{\beta\mu}{2}E_3 + 6\beta\mu'\eta^2E_3,\\
&a = e^{-\beta\varepsilon}, \qquad b = e^{-\beta w}, \qquad d = e^{-\beta w_1};
\end{aligned}$$

$4\nu_c = J_{11}(0) + 2J_{12}(0) + J_{13}(0)$ is the eigenvalue of the long-range interactions matrix Fourier transform $J_{ff'} = \sum_{\mathbf{R}_q-\mathbf{R}_{q'}} J_{ff'}(qq')$; $\beta = 1/k_BT$.

The thermodynamic potential is then obtained in the following form

$$\begin{aligned}
G \;=\; & \frac{v}{2}c_{66}^{E0}\varepsilon_6^2 - ve_{36}^0\varepsilon_6E_3 - \frac{v}{2}\chi_{33}^{\varepsilon 0}E_3^2 + 2\nu_c\eta^2 + 16\mu'E_3\eta^3\\
&+\frac{2}{\beta}\ln 2 - \frac{2}{\beta}\ln\left(1-\eta^2\right) - \frac{2}{\beta}\ln D - v\sigma_6\varepsilon_6.
\end{aligned} \tag{7}$$

Here, σ_6 is the formally introduced shear stress conjugate to the strain ε_6. In numerical calculations we put $\sigma_6 = 0$. The condition of the thermodynamic potential minimum

$$\left(\frac{\partial G}{\partial\varepsilon_6}\right)_{T,E_3,\sigma_6} = 0$$

yields an equation for the strain ε_6

$$\sigma_6 = c_{66}^{E0}\varepsilon_6 - e_{36}^0E_3 + \frac{4\psi_6}{v}\eta + \frac{2r}{vD}. \tag{8}$$

In the same way, we derive the expressions for polarization P_3 and molar entropy of the proton subsystem

$$P_3 = -\frac{1}{v}\left(\frac{\partial G}{\partial E_3}\right)_{T,\sigma_6} = e_{36}^0\varepsilon_6 + \chi_{33}^{\varepsilon 0}E_3 + 2\frac{\mu}{v}\eta + 8\frac{\mu'}{v}\eta^3, \tag{9}$$

$$S = -\frac{N_A}{2}\left(\frac{\partial G}{\partial T}\right)_{E_3,\sigma_6} = R\left[-\ln 2 + \ln(1-\eta^2) + \ln D + 2Tz_T\eta + \frac{M}{D}\right]. \tag{10}$$

Here, N_A is the Avogadro number; R is the gas constant. The following notations are used:

$$\begin{aligned}
&r = -\delta_sM_s - \delta_aM_a + \delta_1M_1,\\
&z_T = -\frac{1}{k_BT^2}(\nu_c\eta - \psi_6\varepsilon_6 + 6\mu'\eta^2E_3),
\end{aligned}$$

$$M = 4b\beta w \cosh(z - \beta\delta_1\varepsilon_6) + \beta w_1 d + 2a\beta\varepsilon \cosh\beta\delta_a\varepsilon_6 + \beta\varepsilon_6 r,$$
$$M_a = 2a\sinh\beta\delta_a\varepsilon_6, M_s = \sinh(2z + \beta\delta_s\varepsilon_6), M_1 = 4b\sinh(z - \beta\delta_1\varepsilon_6).$$

Expressions for dielectric susceptibilities, piezoelectric coefficients, and elastic constants derived [17] from equations (8), (9) are slightly different from the previous ones [10], where the dependence of the effective dipole moment on the order parameter was not taken into account. Numerical calculations, however, showed [17] that in zero electric field the difference is minor.

The molar specific heat of the subsystem described by the Hamiltonian (1) is

$$\Delta C^{\sigma} = T\left(\frac{\partial S}{\partial T}\right)_{\sigma} = T(S_T + S_\eta \eta_T + S_\varepsilon \varepsilon_T). \tag{11}$$

Here,

$$\begin{aligned} S_T &= \left(\frac{\partial S}{\partial T}\right)_{P_3,\varepsilon_6} = \frac{R}{DT}\left[2Tz_T(q_6 - \eta M) + N_6 - \frac{M^2}{D}\right], \\ S_\eta &= \left(\frac{\partial S}{\partial \eta}\right)_{\varepsilon_6,T} = \frac{2R}{D}\left[DTz_T + (q_6 - \eta M)z_\eta\right], \\ S_\varepsilon &= \left(\frac{\partial S}{\partial \varepsilon_6}\right)_{\eta,T} = \frac{R}{DT}\left[-2\left(q_6 - \eta M\right)\psi_6 - \lambda + \frac{M}{D}r\right]. \end{aligned} \tag{12}$$

Notations introduced here are described in appendix.

Then, the total specific heat is

$$C = \Delta C^{\sigma} + C_{\text{regular}}. \tag{13}$$

Here, ΔC^{σ} is assumed to describe all the anomalies of the specific heat at the phase transition, whereas the regular background contribution to the specific heat, mostly from the lattice of heavy ions, is approximated by a linear temperature dependence

$$C_{\text{regular}} = C_0 + C_1(T - T_{\text{c}}). \tag{14}$$

As will be discussed later, this linear approximation agrees with the experimental data.

Finally, the electrocaloric temperature change is calculated using the known formula

$$\Delta T = \int_0^{E_3} \frac{TV}{C}\left(\frac{\partial P_3}{\partial T}\right)_E \mathrm{d}E_3, \tag{15}$$

where the pyroelectric coefficient is

$$\left(\frac{\partial P_3}{\partial T}\right)_E = e^0_{36}\varepsilon_T + \frac{2(\mu + 12\mu'\eta^2)}{v}\eta_T, \tag{16}$$

$V = vN_{\text{A}}/2$ is the molar volume.

3. Numerical calculations

To perform the numerical calculations we need to set the values of the following theory parameters:

- the Slater energies ε, w, w_1;
- the parameter of the long-range interactions ν_{c};
- the effective dipole moment μ and the correction is due to proton ordering μ';
- the deformation potentials ψ_6, δ_s, δ_a, δ_1;

— the “seed” dielectric susceptibility $\chi_{33}^{\varepsilon 0}$, elastic constant c_{66}^{E0}, piezoelectric coefficient e_{36}^{0};

— the parameters of the lattice specific heat C_0 and C_1.

They are chosen, obviously, by fitting the theoretical thermodynamic characteristics to the experimental data, as described in [12]. The obtained optimum sets of the model parameters are given in table 1.

To describe crystals with different deuteration levels, we use the mean crystal approximation, where the theory parameters are assumed to be linearly dependent on deuteron concentration (except for the parameter ν_c, for which a small deviation from the linear dependence is assumed, as it is chosen from the condition that the calculated transition temperature coincides with the experimental one, which is also slightly non-linear). The dependence of the energy levels and interparticle interaction constants on deuteration is caused by the corresponding geometrical changes in the crystal structure with deuteration (elongation of the hydrogen bonds, changes in the distance between the equilibrium positions of H or D on the bonds, changes in the lattice constants, etc).

Table 1. The optimum sets of the model parameters for different crystals. As KD_2PO_4 we denoted $K(H_{1-x}D_x)_2PO_4$ with $x = 0.89$.

	T_c^0 (K)	ε/k_B (K)	w/k_B (K)	ν_c/k_B (K)	μ (10^{-30} C·m)	μ' (10^{-30} C·m)	χ_{33}^0
KH_2PO_4	122.22	56.00	430.0	17.55	5.6	−0.217	0.75
KD_2PO_4	211.73	85.33	730.4	39.26	6.8	−0.217	0.39
KH_2AsO_4	97	35.50	385.0	17.43	5.5	−0.033	0.7
KD_2AsO_4	162	56.00	690.0	31.72	7.3	−0.000	0.5

	ψ_6/k_B (K)	δ_s/k_B (K)	δ_a/k_B (K)	δ_1/k_B (K)	c_{66}^{E0} (10^9 N/m^2)	e_{36}^0 (C/m^2)	C_0 J/(mol K)	C_1 J/(mol K^2)
KH_2PO_4	−150.00	82.00	−500.00	−400.0	7.00	0.0033	60	0.32
KD_2PO_4	−139.89	48.64	−1005.68	−400.0	6.39	0.0033	93	0.32
KH_2AsO_4	−170.00	130.00	−500.0	−500.0	7.50	0.01	60	0.32
KD_2AsO_4	−160.00	120.00	−800.0	−500.0	6.95	0.01	98	0.40

The primitive cell volume is taken to be $v = 0.1946 \cdot 10^{-21}$ cm^3 for $K(H_{1-x}D_x)_2PO_4$ and $v = 0.202 \cdot 10^{-21}$ cm^3 for $K(H_{1-x}D_x)_2AsO_4$, irrespectively of the deuteration. The energy w_1 of proton configurations with four or zero protons near the given oxygen tetrahedron should be much higher than ε and w. Therefore, we take $w_1 = \infty$ $(d = 0)$.

As we have already mentioned, when the dependence of the effective dipole moment on the order parameter is taken into account, the agreement between the theory and experiment for most of the calculated dielectric, piezoelectric, elastic characteristics, and specific heat of the studied crystals in the absence of an external electric field is neither improved nor worsened (see [17]). However, the present model allows us to describe more consistently the smearing of the first order phase in high electric fields.

The temperature dependence of the specific heat of KH_2PO_4 and KD_2PO_4 is shown in figure 1. The contribution ΔC^{σ} is essential in the transition region and satisfactorily describes the experimental anomalies. As one can see, the total specific heat above T_c can be well approximated by a linear temperature dependence, thus justifying the linear dependence of C_{regular}, given by equation (14).

In figures 2 and 3 we plotted the temperature variation of polarization of $K(H_{1-x}D_x)_2PO_4$ in different fields. The agreement with experiment is better at $x = 0.89$ (and 0.84, see [17]) than at $x = 0$. We believe this is due to proton tunnelling, essential in non-deuterated samples, which is not included in our model.

The field E_3, which in these crystals is the field conjugate to the order parameter, induces non-zero polarization P_3 above the transition point. Polarization has a jump at T_c, indicating the first order phase transition. With an increasing field, the polarization jump decreases, whereas the transition temperature T_c increases almost linearly. The corresponding $\partial T_c/\partial E_3$ slopes are 0.192 and 0.115 K cm/kV for $x = 0$

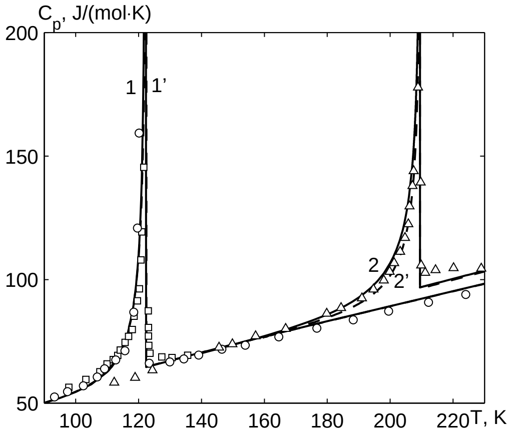

Figure 1. The temperature dependence of the molar specific heat of $K(H_{1-x}D_x)_2PO_4$ at $x = 0.0$ — ○ [18], ☐ [19]; at $x = 0.86$ — △ [19]. Dashed lines 1' and 2': the theoretical results of [12].

and $x = 0.89$, respectively (c.f. 0.22 and 0.13 K cm/kV from our earlier calculations [10] and experimental 0.125 K cm/kV of [23] for $x = 0.89$). At some critical field E^*, the jump vanishes, and the transition smears out. The calculated coordinates of the critical point are $E^* = 125$ V/cm, T_c^*=122.244 K for $x = 0$ and 7.1 kV/cm, 212.55 K for $x = 0.89$, which agrees well with the experiment [22, 23]. It should be noted that in our previous calculations [12] it was impossible to obtain a correct description of the polarization behavior in the fields above the critical one, due to the necessity of using two different values of the effective dipole moment μ in calculations.

The calculated electrocaloric changes of temperature ΔT of the $K(H_{1-x}D_x)_2PO_4$ and $K(H_{1-x}D_x)_2AsO_4$ crystals with the adiabatically applied electric field are shown in figures 4 and 5. The experimental data of [7] were obtained at $T = 121$ K, which was very close to the transition temperature of the sample used in the measurements.

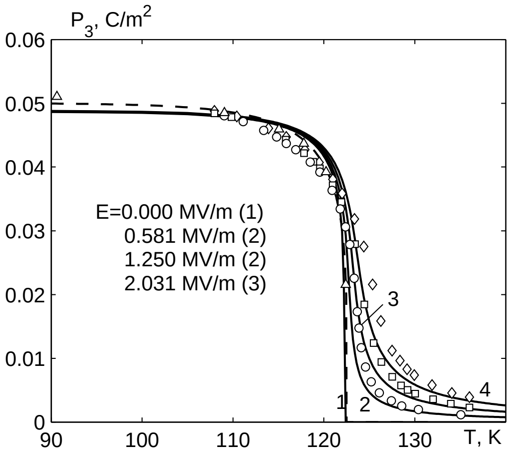

Figure 2. The temperature dependence of polarization of KH_2PO_4 at different E_3(MV/m): 0.0 — 1, △ [5]; 0.581 — 2, ○ [20]; 1.250 — 3, ☐ [20]; 2.031 — 4, ◊ [20]. Symbols are experimental points; solid lines: the present theory; dashed lines: the theoretical results of [12].

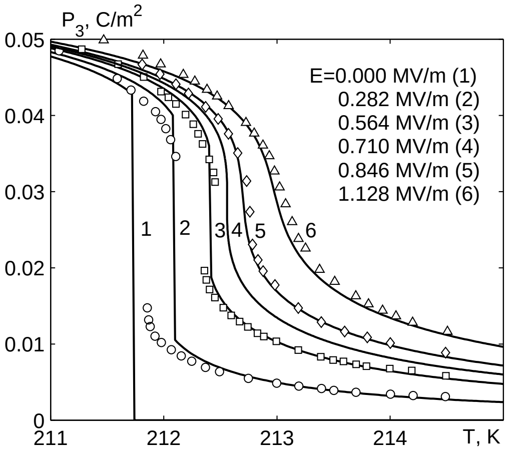

Figure 3. The temperature dependence of polarization of $K(H_{1-x}D_x)_2PO_4$ at $x = 0.89$ and at different E_3 (MV/m): 0.0 — 1; 0.282 — 2, ○; 0.564 — 3, ☐; 0.71 — 4; 0.846 — 5, ◊; 1.128 — 6, △. Symbols are experimental points taken from [21]; lines: the present theory.

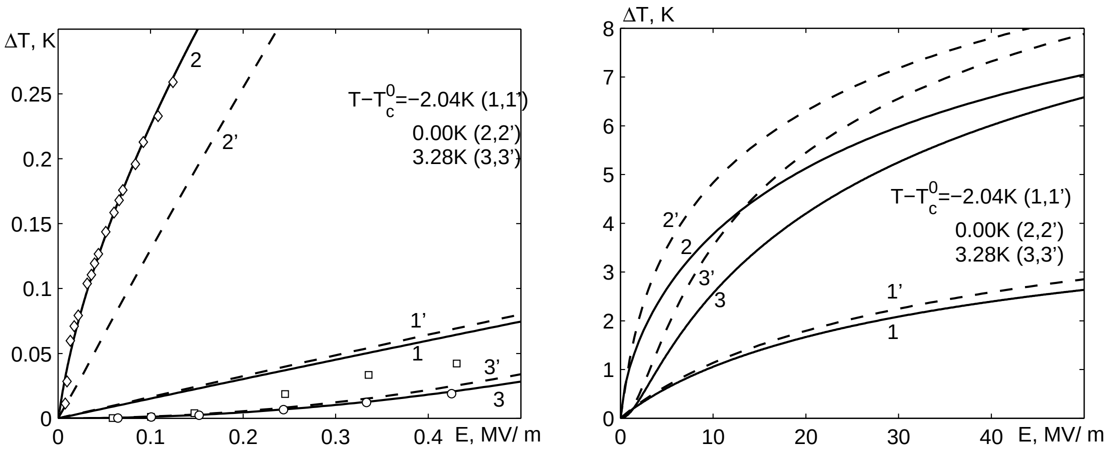

Figure 4. The field dependence of the electrocaloric temperature change of $K(H_{1-x}D_x)_2PO_4$ for $x = 0.0$ (solid lines) and $x = 0.89$ (dashed lines) at $T - T_c^0 = -2.04$ K — 1, 1′, □; $T = T_c^0$ — 2, 2′, ∘; $T - T_c^0 = 3.2$ K — 3, 3′, ⋄. Experimental points are taken from [5] — ∘, □ and [7] — ⋄.

As one can see, at small fields (figures 4, 5, left-hand) the calculated electrocaloric temperature change is a linear function of the field below T_c^0 (curves 1, 1′) and a quadratic function above T_c^0 (at 2, 2′). The experimental behavior below T_c^0 is not linear at $E_3 < 2$ kV/cm due to the domains: The domains, whose polarization is oriented along the field, are heated, whereas the domains, polarized in the opposite direction are cooled, thus the resulting net change of the sample temperature is close to zero. The experimental data for the electrocaloric temperature change at and above T_c^0 available for KH_2PO_4, as well as the $\Delta T/\Delta E$ ratio below T_c^0 at fields above 2 kV/cm (when the sample is in a single-domain state), are well reproduced by the theory.

At higher fields (figures 4, 5, right-hand) the calculated electrocaloric temperature changes at temperatures above T_c^0 are larger than below T_c^0. The obtained curves deviate from linear and quadratic behavior and reach saturation at $E \gg 500$ kV/cm. It should be mentioned, however, that these curves are calculated with the linear over the field E_3 pseudospin Hamiltonian (3). It would be very interesting to compare our results at high fields with experiment, for instance, to find out when non-linear contributions to the Hamiltonian cannot be omitted any longer. Unfortunately, no experimental data for ΔT in

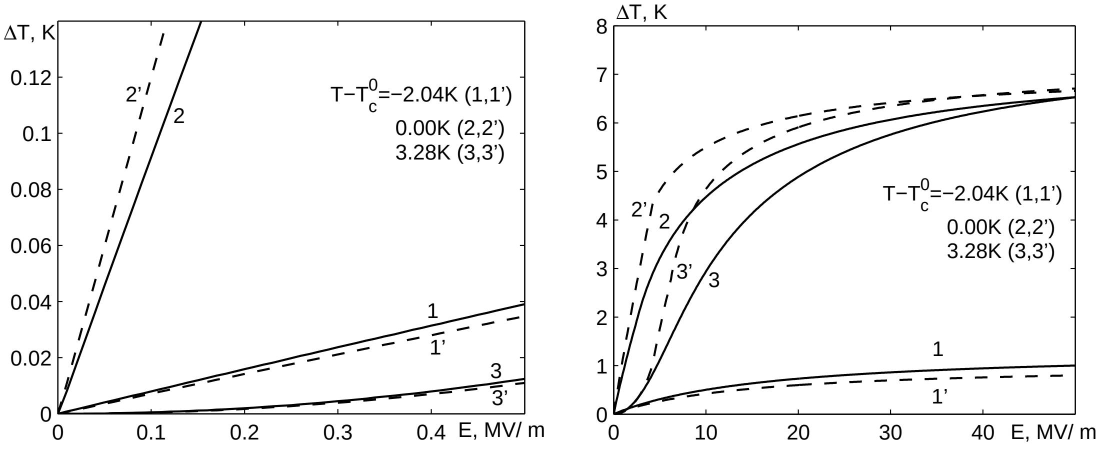

Figure 5. The field dependence of the electrocaloric temperature change of KH_2AsO_4 (solid lines) and KD_2AsO_4 (dashed lines) at $T - T_c^0 = -2.04$ K — 1, 1′; $T = T_c^0$ — 2, 2′; $T - T_c^0 = 3.2$ K — 3, 3′.

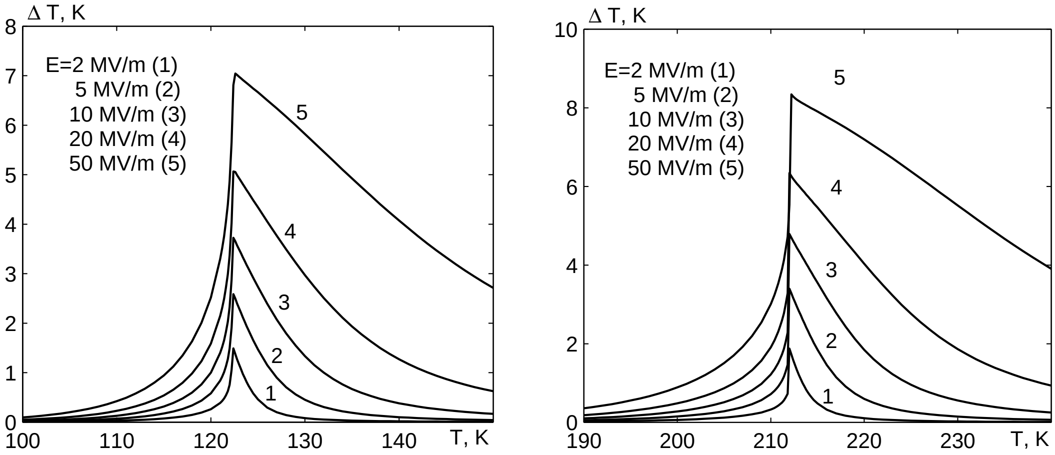

Figure 6. The temperature dependence of the electrocaloric temperature change of $K(H_{1-x}D_x)_2PO_4$ for $x = 0.0$ (left-hand) and $x = 0.89$ (right-hand) in different fields.

the fields above 1 kV/cm are available. And, of course, possibilities for experimental measurements are limited by the dielectric strength of the samples.

As one can see from the temperature dependence of ΔT (figure 6) for $K(H_{1-x}D_x)_2PO_4$ crystals, the calculated electrocaloric temperature change is the largest at temperatures below T_c^0 but close T_c and can exceed 6 K; however, the fields required to reach ΔT that high are not accessible in reality, because most likely they exceed the dielectric strength of the crystals.

4. Conclusions

Taking into account the dependence of the effective dipole moment on the order parameter within the framework of the proton ordering model allows us to correctly describe the smearing of the ferroelectric phase transition in high electric fields as well as the electrocaloric effect in the KDP family crystals. The theory predicts the values of the electrocaloric temperature change of a few Kelvins in high fields. Additional experimental measurements of ΔT in the fields above 2 kV/cm are necessary.

Appendix

The notations introduced in equations (11)–(12) are as follows:

$$\begin{aligned} N_6 \quad = \quad & 2a(\beta\varepsilon)^2\cosh\beta\delta_a\varepsilon_6 + 4b(\beta w)^2\cosh(z-\beta\delta_1\varepsilon_6) + (\beta w_1)^2 d + 2\varepsilon_6\beta^2(-\varepsilon\delta_a M_a + w\delta_1 M_1) \\ & + \varepsilon_6^2\left[2a(\beta\delta_a)^2\cosh\beta\delta_a\varepsilon_6 + (\beta\delta_s)^2\cosh(2z+\beta\delta_s\varepsilon_6) + 4b(\beta\delta_1)^2\cosh(z-\beta\delta_1\varepsilon_6)\right], \end{aligned}$$

$$q_6 = 2b\beta w\sinh(z-\beta\delta_1\varepsilon_6) + \varepsilon_6\beta\left[-\delta_s\cosh(2z+\beta\delta_s\varepsilon_6) + 2b\delta_1\cosh(z-\beta\delta_1\varepsilon_6)\right],$$

$$\lambda = -\beta\varepsilon\delta_a M_a + \beta w\delta_1 M_1 + \varepsilon_6\beta\left[\delta_s^2\cosh(2z+\beta\delta_s\varepsilon_6) + 2a\delta_a^2\cosh\beta\delta_a\varepsilon_6 + 4b\delta_1^2\cosh(z-\beta\delta_1\varepsilon_6)\right],$$

$$\eta_T = p_6^\varepsilon + \frac{v}{2(\mu+12\mu'\eta^2)}(e_{36}-e_{36}^2)\varepsilon_T,$$

$$\varepsilon_T = \left[\frac{2\beta}{vD}\left(2Tz_T f_6 - \lambda + \frac{Mr}{D}\right) - \frac{4p_6^\varepsilon}{v}\left(\psi_6 - \frac{z_\eta f_6}{D}\right)\right] \Big/ c_{66}^E.$$

In turn,

$$p_6^\varepsilon = \frac{1}{T}\frac{2\varkappa Tz_T + [q_6 - \eta M]}{D - 2\varkappa z_\eta},$$

c_{66}^{E} is the isothermal elastic constant at a constant field

$$\begin{aligned} c_{66}^{E} &= c_{66}^{E0} + \frac{8\psi_6}{v}\frac{\beta(-\psi_6\varkappa + f_6)}{D-2z_\eta\varkappa} - \frac{4\beta z_\eta f_6^2}{vD(D-2z_\eta\varkappa)} \\ &\quad - \frac{2\beta}{vD}\left[\delta_s^2\cosh(2z+\beta\delta_s\varepsilon_6) + 2a\delta_a^2\cosh\beta\delta_a\varepsilon_6 + 4b\delta_1^2\cosh(z-\beta\delta_1\varepsilon_6)\right] + \frac{2\beta r^2}{vD^2}\,, \end{aligned}$$

and e_{36} is the isothermal piezoelectric coefficient

$$e_{36} = -\left(\frac{\partial\sigma_6}{\partial E_3}\right)_{T,\varepsilon_6} = \left(\frac{\partial P_3}{\partial\varepsilon_6}\right)_{T,E_3} = e_{36}^{0} + \frac{2(\mu+12\mu'\eta^2)}{v}\frac{\beta\theta_6}{D-2z_\eta\varkappa}\,,$$

with

$$\begin{aligned} &\theta_6 = -2\varkappa\psi_6 + f_6\,, \qquad f_6 = \delta_s\cosh(2z+\beta\delta_s\varepsilon_6) - 2b\delta_1\cosh(z-\beta\delta_1\varepsilon_6) + \eta r, \\ &z_\eta = \frac{1}{1-\eta^2} + \beta\nu_{\mathrm{c}} + 12\beta\mu'\eta E_3\,. \end{aligned}$$

References

1. Valant M., Progr. Mater. Sci., 2012, **57**, 980; doi:10.1016/j.pmatsci.2012.02.001.
2. Scott J.F., Annu. Rev. Mater. Res., 2011, **41**, 229; doi:10.1146/annurev-matsci-062910-100341.
3. Mischenko A.S., Zhang Q., Scott J.F., Whatmore R.W., Mathur N.D., Science, 2006, **311**, 1270; doi:10.1126/science.1123811.
4. Rose M.C., Cohen R.E., Phys. Rev. Lett., 2012, **109**, 187604; doi:10.1103/PhysRevLett.109.187604.
5. Wiseman G.G., IEEE Trans. Electron Devices, 1969, **16**, 588; doi:10.1109/T-ED.1969.16804.
6. Baumgartner H., Helv. Phys. Acta., 1950, **23**, 651.
7. Shimshoni M., Harnik E., J. Phys. Chem. Solids, 1969, **31**, 1416; doi:10.1016/0022-3697(70)90148-4.
8. Dunne L.J., Valant M., Manos G., Axelsson A.-K., Alford N., Appl. Phys. Lett., 2008, **93**, 122906; doi:10.1063/1.2991443.
9. Slater J.C., J. Chem. Phys., 1941, **9**, 16; doi:10.1063/1.1750821.
10. Stasyuk I.V., Levitskii R.R., Moina A.P., Lisnii B.M., Ferroelectrics, 2001, **254**, 213; doi:10.1080/00150190108215002.
11. Stasyuk I.V., Levitskii R.R., Zachek I.R., Moina A.P., Phys. Rev. B, 2000, **62**, 6198; doi:10.1103/PhysRevB.62.6198.
12. Levitsky R.R., Zachek I.R., Vdovych A.S., Moina A.P., J. Phys. Stud., 2010, **14**, 1701.
13. Lisnii B.M., Levitskii R.R., Baran O.R., Phase Transitions, 2007, **80**, 25; doi:10.1080/01411590701315591.
14. Stasyuk I.V., Levitskii R.R., Phys. Status Solidi B, 1970, **39**, K35; doi:10.1002/pssb.19700390144.
15. Levitskii R.R., Korinevski N.A., Stasyuk I.V., Ukr. J. Phys., 1974, **19**, 1289.
16. Blinc R., Svetina S., Phys. Rev., 1966, **147**, 430; doi:10.1103/PhysRev.147.430.
17. Vdovych A.S., Moina A.P., Levitskii R.R., Zachek I.R., Preprint arXiv:1405.1327, 2014.
18. Stephenson C.C., Hooly G.J., J. Am. Chem. Soc., 1944, **66**, No. 8, 1397; doi:10.1021/ja01236a054.
19. Strukov B.A., Baddur A., Koptsik V.A., Velichko I.A., Solid State Phys., 1972, **14**, No. 4, 1034.
20. Chabin M., Gilletta F., Ferroelectrics, 1977, **15**, 149; doi:10.1080/00150197708237808.
21. Sidnenko E.V., Gladkii V.V., Kristallografiya, 1972, **17**, 978 (in Russian) [Sov. Phys. Crystallogr., 1973, **17**, 861].
22. Western A.B., Baker A.G., Bacon C.R., Schmidt V.H., Phys. Rev. B, 1978, **17**, 4461; doi:10.1103/PhysRevB.17.4461.
23. Gladkii V.V., Sidnenko E.V., Sov. Phys. Solid State, 1972, **13**, 2592.

Електрокалоричний ефект у кристалах типу KH_2PO_4

А.С. Вдович[1], А.П. Моїна[1], Р.Р. Левицький[1], І.Р. Зачек[2]

[1] Інститут фізики конденсованих систем НАН України, вул. І. Свєнціцького, 1, 79011 Львів, Україна

[2] Національний університет “Львівська політехніка”, вул. С. Бандери, 12, 79013 Львів, Україна

В моделі протонного впорядкування для кристалів типу KH_2PO_4 враховано залежність ефективних дипольних моментів від параметра протонного впорядкування. В наближенні чотиричастинкового кластера розраховано поляризацію кристалів та досліджено електрокалоричний ефект у них. Описано розмивання сегнетоелектричного фазового переходу поздовжним електричним полем. Отримано добре узгодження з експериментальними даними.

Ключові слова: *електрокалоричний ефект, KDP, кластерне наближення, поляризація*